Intrapixel Health Monitoring by Coupled Spontaneous Emission in Small-Pitch Flip-Chip-Bonded 10-Gbit/s 2-D VCSEL Arrays

Hendrik Roscher

In an effort to create architectures of high element-count vertical-cavity surface-emitting laser (VCSEL) arrays that are forgiving of a limited number of device failures, we have demonstrated pixel designs with redundancy of sources. The new pixel consists of three identical, individually addressable lasers that are flip-chip bonded directly to the device mesas. All VCSELs in a pixel share some mirror layers that serve to couple a fraction of spontaneous emission between them. Spontaneous emission is a function of carrier density, and carrier density above threshold a measure of the total losses in the structure. The generated photocurrent in idle devices of the same pixel can hence be employed to detect degradation in the transmitting laser. This is a novel scheme of efficient transmitter-side monitoring in individual channels without intercepting coherent emission, and without integration of extra monitor photodiodes that would jeopardize compactness and low-cost fabrication.

We have implemented a redundant pixel architecture for 850 nm wavelength, 10-Gbit/s serial data rate, two-dimensional (2-D) VCSEL arrays [1] as a possible cost-efficient solution to VCSEL reliability concerns in increasingly emerging high element-count array applications [2], [3]. Following a sparing strategy, the new pixel consists of three identical lasers instead of one. The additional VCSELs are there to monitor the transmitting laser, and to expeditiously replace it in case of failure or undue degradation.

Redundancy is a powerful method to improve reliability. Yet, with alternative laser sources available in each channel, the arising question is how a VCSEL failure can be detected. The driver circuit should be able to respond to a failure by permanently switching to one of the backup VCSELs held in reserve in each channel. An apparent but perhaps less elegant solution is to employ a separate feedback channel over which the receiver signals the non-functioning channel to the transmitter. Clearly, there is a need for VCSEL health monitoring directly on the transmitter side of an optical data link.

External monitor diodes are generally used for dynamic power stabilization in solitary devices, but cannot distinguish between individual channels of high-density arrays. There have been several publications of monolithic integration of monitor diodes with VCSEL structures, both as extra-cavity structures intercepting the light output [4] or as intracavity quantum well absorbers [5]. However, the integration of absorbing elements with the laser structure interferes with its optical properties and entails a more complex fabrication (growth of additional epitaxial layers and extra fabrication steps) of these three-terminal devices. Another possibility is to flip-chip bond the VCSEL array to a corresponding

array of photodiodes to monitor the residual back emission [6]. This, however, precludes direct-mesa bonding needed for thermal management.

All the aforementioned implementations aim for a linear photocurrent response to the coherent laser emission as a direct measure of the output power, for instance, to insure that eye safety limits are not exceeded. However, to a greater or lesser extent, the detectors are also sensitive to the spontaneous emission, and the recorded signals need to be corrected for this in order to give an accurate measure of the output power.

The present pixel design follows a different approach: Instead of measuring the coherent output we access internal data, namely the carrier density via spontaneous emission. As one of the key internal parameters for lasing operation, this will provide just as valuable status information concerning degradation. The excess carrier density in the active region of a laser diode above threshold assumes a value that corresponds to the total losses in the structure. It may hence be used as a measure of degradation.

To this end, we have implemented a pixel structure that allows mutual monitoring between equal VCSELs by coupled spontaneous emission. Figure 1 displays the pixel in a schematic cross-section that includes two of three VCSELs. The three-laser pixels are hybridized onto a silicon development platform via flip-chip bonding to emulate a typical configuration where optical sources are mated with, e.g., CMOS compatible electronics. While the fabrication details are explained elsewhere [1], this technology relies on the following capabilities: self-aligned top contact formation, dry etching to produce vertical mesa sidewalls of marginal roughness, lateral oxidation for current confinement, a flip-chip process utilizing non-planar bond pads along with elongated and compressed bumps to prevent shorts, and, eventually, complete substrate removal to define the outcoupling facets.

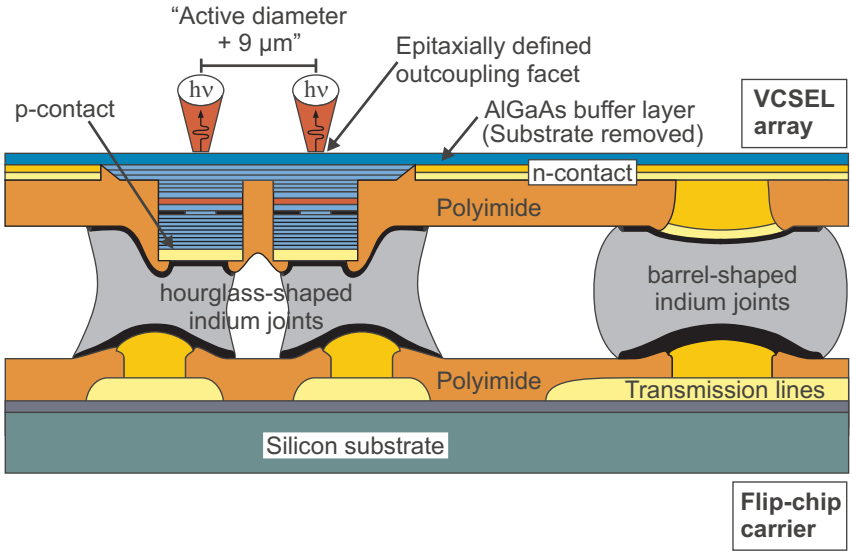

Fig. 1: Schematic cross-section of the complete pixel, including densely packed direct-mesa bonded VCSELs with common n-type mesa and solder joints of reduced cross-section preventing electrical shorts between individually addressable lasers [1].

This last step also produces a structure resembling a planar waveguide that is composed of stacked epitaxial mirror and current injection layers of about 5 to 6 µm total thickness. The lasers are connected by this waveguide in the lateral direction just beneath the inner cavities. The structure of separate close-spaced top mesas sitting on a shared bottom mesa is essentially a structure of pn-junctions coupled to a film waveguide. Without substrate, a major source of thermal crosstalk is eliminated. However, these devices now lack a natural heat spreader that distributes dissipated heat over a large surface area from where it can then be removed by convection.

The design aims at closest possible center-to-center distances for mesa-isolated VCSELs while maintaining good thermal and dynamic characteristics. For device thermal management, the solder balls are placed over the mesas to create alternate paths for outflow of heat, allowing high-current VCSEL operation without excessive internal heating. Tight thermal coupling of each laser via the solder joints to the adjacent substrate also diminishes the parasitic thermal coupling caused by the shared planar waveguide whose actual function is optical coupling of spontaneous emission.

The measurements displayed in Fig. 2 show that the idle backup VCSELs in the pixel receive a fraction of incoherent radiation coming from the emitting laser. The photocurrent behavior in one of the two unbiased VCSELs against the laser current of the operating VCSEL resembles the expected behavior of the carrier density inside the laser. The light–current–voltage (LIV) curves were independently recorded with a computer-controlled setup. The photocurrent curve is obtained by manually taking the values from an ampere meter every 0.5 mA. In this case, the recording of those values was stopped at roll-over of

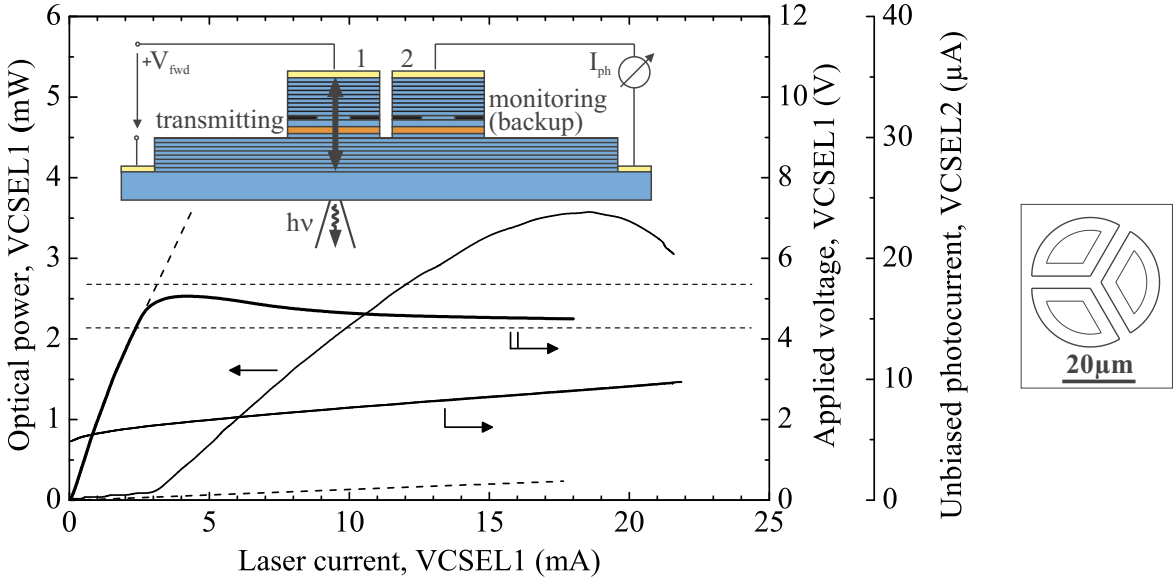

Fig. 2: LIV curves of VCSEL 1 and corresponding unbiased photocurrent I_{ph} of VCSEL 2 of the same pixel. These VCSELs are wedge-shaped with active areas of about 84 µm^2, mesas are separated in this case by a 3.3 µm wide trench. The schematic on the right is a true-to-scale representation of this pixel. A more detailed description of wedge VCSELs is provided in [7]. The dashed lines are explained in the text.

the LI curve since this fully covers the practically relevant operation range of the VCSELs.

While the total rate of recombination processes below threshold is directly proportional to current density, the actual increase in excess carrier densities with current density is slower than linear because the lifetime of carriers becomes ever shorter as their numbers grow. Spontaneous emission is what ignites lasing. In a perfect gain region of a laser, all injected carriers are turned into suitable photons through bimolecular recombination (which is predominantly radiative in a direct bandgap semiconductor). There are, however, unwanted competing recombination channels that consume part of the carriers and eventually only add to heat generation rather than providing optical gain. Non-radiative multi-particle processes such as Auger recombination by nature become more likely as particle densities go up. Hence they take away an ever greater portion of the injected current as it is increased.

The photocurrent reading is a result only of the wanted radiative recombination, and the fact that an increasing part of the current flows through non-radiative channels as threshold is approached expresses itself in a continuous decline of the slope. It should be mentioned that part of the spontaneous emission is likely to come from the barrier layers surrounding the active quantum wells which to some extend will escape fundamental absorption (with the possibility of subsequent recycling) in lower bandgap mirror layers. In Fig. 2, the photocurrent below threshold shows, however, only a relatively minor deviation from a straight line which indicates a high internal efficiency of the device.

The total recombination rate $R_{\mathrm{tot}} \propto j$ is the sum of radiative and non-radiative processes, $R_{\mathrm{tot}} = R_{\mathrm{r}} + R_{\mathrm{nr}}$, where $R_{\mathrm{r}} \propto n^2$ (two-particle process) and $R_{\mathrm{nr}} \propto n^3$ (three-particle Auger process), j is the current density and n the excess carrier density. The latter proportionality is true when non-radiative recombination via traps (intermediate level states) is neglected. Recombination via traps possesses a lifetime that is linked to the trap nature and is thus independent of carrier density, leading to a linear increase of both carrier density and recombination rate with current density.

It is noted that this analysis assumes there are no geometric effects to alter the received portion of spontaneous emission through spatial redistribution of carrier densities while the current is being increased up to threshold. Below threshold this seems reasonable, since current crowding effects should be negligible at low currents, and there is also no spatially varying mode pattern to interact with the carrier distribution. Furthermore, within the limited current range under consideration, the carrier injection efficiency is assumed constant. Reference [8] provides a more in-depth treatment how nonradiative recombination can be investigated through lateral spontaneous emission.

The situation changes on reaching threshold, where onset of lasing provides an extremely efficient mechanism to instantly convert additionally injected carriers into photons of the lasing modes. The carrier density is thereby effectively pinned to the value that corresponds to the total amount of optical losses in the laser. A combination of several factors may cause the decline of photocurrent beyond threshold that is nevertheless observed in Fig. 2. One mechanism is the positive temperature coefficient of the mirror contrast, namely the refractive index step between alternating distributed Bragg reflector layers in the mirrors, $\partial \Delta \bar{n} / \partial T > 0$. It works to reduce the mirror losses and hence the carrier density above threshold when the internal temperature rises.

However, other temperature-dependent properties like the gain-to-resonance detuning and carrier heating may also interfere. Especially for multimode VCSELs, the modal structure will change considerably with laser current. Its interplay with the spatial and spectral carrier distributions will alter the number of carriers contributing to spontaneous emission. And after all there is no certainty whether the sensing device receives a constant portion of the total emitted incoherent radiation. A spatial variation of the charge distribution caused, for instance, by current crowding and spatial hole burning might well lead to a varying degree of radiation shielding by the trench between devices.

Figure 3 demonstrates in the right hand part how the spontaneous emission is distributed within a pixel. The bright spot in the center is surface-normal emission from the outcoupling facet of the forward-biased VCSEL. It is driven below threshold here, so the weak lateral radiation can be observed. On the left, the figure shows the mesa structure that is, in a flipped-over position according to Fig. 1, on the underside of that pixel. This scan is prior to flip-chip packaging and substrate removal. The three small mesas define the substrate-side emitting VCSELs, dry-etched through the active layers to a depth of 6 µm and separated by 1.5 µm at the smallest distance.

There is weak radiation from the edges of the shared epitaxial layers that gives evidence of guided spontaneous emission. Apparently, the wet-etched bottom mesa with its epitaxial layers is acting as a waveguide in the lateral direction. Wave propagation inside a similarly layered structure has already been reported in [9]. The observed emission from the edges of the large bottom mesa suggests that this sensor function could work over larger device-to-device spacings than implemented in this work. The two especially dark circular areas adjacent to the bright spot of the emitting VCSEL in Fig. 3 reveal the position of the two unbiased VCSELs where the radiation is leaking from the shared waveguide in the vertical direction going into the plane of the paper. This generates a photocurrent in the pn-junctions of those backup VCSELs.

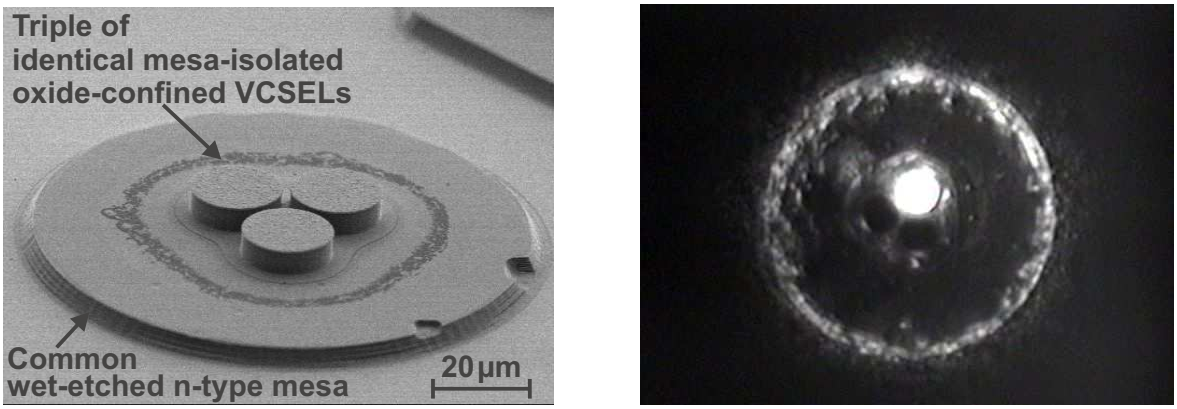

Fig. 3: Scanning electron micrograph (SEM) showing the multi-mesa structure on the underside of a pixel prior to flip-chip packaging and substrate removal (left), and CCD image showing a pixel from the emission side, one VCSEL forward biased far below threshold to demonstrate the distribution of spontaneous emission (right).

We envision that through this behavior, the health of the operating VCSEL can be monitored by at least one of the backup VCSELs in the same pixel. Evaluation of the photocurrent signal will allow to judge whether the transmitting laser is operating within specified parameters. This function is provided with no added complexity to the VCSEL structure and no interference with the coherent emission.

The detection of spontaneous lateral emission has been reported in [10] and [11] with top-emitting VCSEL structures. The detector in [10] is etched through all epitaxial layers to the substrate, so detector and VCSEL do not share any layers. The substrate is not removed and there is a much larger, 30 µm-wide gap between the one VCSEL in the center and a dedicated detector ring enclosing it. The photocurrent of this detector does not saturate and only shows a small slope change at threshold. Besides onset of lasing only in a small portion of the active region there could also be scattering from the sidewalls of those early air-post VCSELs or even from the backside of the substrate such that a fraction of stimulated emission is also detected. Reference [11] in contrast exploits in-plane waveguiding of spontaneous emission in the cavity section for long-range monitoring. The active layers connect VCSELs here over distances of 250 µm.

In the present design, the operating and monitor VCSELs are connected by a thin stack of epitaxial layers immediately below the active regions. In this respect, the configuration is similar to [8]. The active layers are fully separated by etching through to the first layers of the bottom Bragg mirror. It is believed that complete substrate removal of these substrate-side-emitting devices also contributes to the suppression of coherent optical crosstalk while the sharing of most of the n-type Bragg layers sufficiently couples the spontaneous emission to result in a photocurrent signal strong enough for monitoring purposes.

It is unclear at this point to what degree the close proximity of the semiconductor–air interface contributes to the lateral coupling or waveguiding. In the absence of total internal reflection at this interface, the distributed Bragg reflector layers could still offer sufficient Bragg reflection for rays incident under an appropriate range of angles. Then this scheme could also be used with on-substrate VCSELs. Coherent crosstalk via the distant semiconductor–air interface at the backside of the substrate should then probably be suppressed by an antireflection coating which is advisable in any case for through-substrate backside emission to avoid the external resonator. A broader band multi-layer antireflection coating might be in order to account for the beam divergence and prevent reflections into laterally displaced backup VCSELs besides the prevention of direct feedback of perpendicular rays into the emitting laser.

In any case, after proper calibration, the excess carrier density in the active region of the operating laser can be observed along with the threshold current. Both are measures of the optical losses in the laser and should give a good indication of its status. Defect formation, diffusion processes of doping species in the Bragg mirrors, facet damage, or simply device failure are examples that would alter the excess carrier density and/or threshold current. In connection with information about the laser current, other problems such as incomplete current injection or current leakage can also be detected.

We suggest that if the photocurrent leaves a predefined band such as indicated in Fig. 2, it can be concluded that the operating VCSEL reached its end of life. In case a laser fails to

lase but still produces spontaneous emission, it essentially works as an LED and there will be no gain clamping. In this case, the carrier density and hence the spontaneous emission will not saturate but continue to increase with the laser current beyond threshold. The photocurrent curve will then leave the predefined band through the top boundary. This is indicated by the dashed line extending the subthreshold part of the photocurrent curve in Fig. 2. At this point, one of the two backup lasers ought to be invoked by the electronics to continue transmission over the affected channel.

Besides detecting VCSEL failure, this function may also provide a means of in-situ monitoring of changes in optical feedback, for instance from the fiber endface, since feedback effectively changes the reflectivity of the outcoupling mirror, hence altering the carrier density. In a real transceiver package, the feedback level may change on a slow time scale, for instance with temperature fluctuations or otherwise induced mechanical stress. Due to their "temporal signature", isolation of the feedback-related changes might be possible. If feedback sensitivity is an issue, the sensor function could proof useful in assessing fiber-pigtailed packages in this respect.

Before deployment in a real transceiver, extensive tests will of course be needed for calibration of the sensor function. Data need to be acquired on how the photocurrent reacts to what mechanism of device aging or failure. Here, we merely demonstrate the principle and explain the potential we see for it. Apart from the described use, another mode of operation is conceivable where all three VCSELs in a pixel are simultaneously transmitting the same signal with a large enough power budget to keep the channel operational as long as one of the VCSELs is still functioning. This approach is attractive in that it largely avoids the added capabilities needed in the driver circuitry to monitor and manage the VCSELs within a pixel, although other difficulties such as synchronization or difference frequency generation at the photodetector might arise.

Thought has to be given to problems such as area-correlated failures in dense arrays which have an impact on the expected extension of lifetime achieved through provisioning of backup devices. We believe that the low power densities in the VCSELs during sensing will not contribute much to their aging, despite the elevation of temperature they undergo because of intra-pixel thermal crosstalk.

Acknowledgment

Special thanks are due to Andrea Kroner and Philipp Gerlach for stimulating discussions regarding the sensor functionality.

References

[1] H. Roscher, F. Rinaldi, and R. Michalzik, "Small-pitch flip-chip bonded VCSEL arrays enabling transmitter redundancy and monitoring in 2-D 10-Gbit/s space-parallel fiber transmission", *IEEE J. Select. Topics Quantum Electron.*, vol. 13, pp. 1279–1289, 2007.

[2] J.E. Cunningham, D.K. McElfresh, L.D. Lopez, D. Vacar, and A.V. Krishnamoorthy, "Scaling vertical-cavity surface-emitting laser reliability for petascale systems", *Appl. Opt.*, vol. 45, pp. 6342–6348, 2006.

[3] N. Mukoyama, H. Otoma, J. Sakurai, N. Ueki, and H. Nakayama, "VCSEL array-based light exposure system for laser printing", in *Vertical-Cavity Surface-Emitting Lasers XII*, C. Lei, J.K. Guenter (Eds.), Proc. SPIE 6908, pp. 69080H-1–11, 2008.

[4] G. Hasnain, K. Tai, Y.H. Wang, J.D. Wynn, K.D. Choquette, B.E. Weir, N.K. Dutta, and A.Y. Cho, "Monolithic integration of photodetector with vertical cavity surface emitting laser", *Electron. Lett.*, vol. 27, pp. 1630–1632, 1991.

[5] G. Steinle, D. Wolf, M. Popp, and K.J. Ebeling, "Vertical-cavity surface-emitting laser monolithically integrated with intracavity monitor diode with temperature-insensitive responsivity", *Electron. Lett.*, vol. 37, pp. 34–36, 2001.

[6] K.W. Goossen, J.E. Cunningham, and A.V. Krishnamoorthy, "1 × 12 VCSEL array with optical monitoring via flip-chip bonding", *IEEE Photon. Technol. Lett.*, vol. 18, pp. 1219–1221, 2006.

[7] H. Roscher, P. Gerlach, F.N. Khan, A. Kroner, M. Stach, A. Weigl, and R. Michalzik, "Toward more efficient fabrication of high-density 2-D VCSEL arrays for spatial redundancy and/or multi-level signal communication", in *Micro-Optics, VCSELs, and Photonic Interconnects II: Fabrication, Packaging, and Integration*, H. Thienpont, M.R. Taghizadeh, P. Van Daele, J. Mohr (Eds.), Proc. SPIE 6185, pp. 61850V-1–12, 2006.

[8] J.-H. Shin and Y.H. Lee, "Determination of nonradiative recombination coefficients of vertical-cavity surface-emitting lasers from lateral spontaneous emission", *Appl. Phys. Lett.*, vol. 67, pp. 314–316, 1995.

[9] A.Y. Cho, A. Yariv, and P. Yeh, "Observation of confined propagation in Bragg waveguides", *Appl. Phys. Lett.*, vol. 30, pp. 471–472, 1977.

[10] K.D. Choquette, N. Tabatabaie, and R.E. Leibenguth, "Detector-enclosed vertical-cavity surface emitting lasers", *Electron. Lett.*, vol. 29, pp. 466–467, 1993.

[11] C. Bringer, V. Bardinal, E. Daran, T. Camps, Y.G. Boucher, G. Almuneau, O. Gauthier-Lafaye, P. Dubreuil, J.-B. Doucet, and C. Fontaine, "Detection of lateral spontaneous emission for VCSEL monitoring", in *Micro-Optics, VCSELs, and Photonic Interconnects*, H. Thienpont, K.D. Choquette, M.R. Taghizadeh (Eds.), Proc. SPIE 5453, pp. 209–216, 2004.